Freeze-Thaw Conditions

Identification

1. Indicator Description

This indicator measures the number of days with unfrozen conditions of the land surface in the contiguous 48 states and Alaska between 1979 and 2019. The balance between frozen and thawed conditions can be an important factor in determining impacts to surface hydrology—including evapotranspiration and the timing and extent of seasonal snowmelt (Kim et al., 2017a). It can also be an important factor in determining the potential growing season for vegetation, which relates to landscape phenological shifts and important impacts on agriculture and natural resource sectors (Weltzin et al., 2020). For instance, some pests and pathogens affecting forests and crops are projected to benefit from warmer temperatures and shorter frozen seasons. A decrease in frozen days may also affect habitat conditions and wildfire risk (USGCRP, 2018).

This indicator focuses on changes in the number of unfrozen days, which is calculated for each year as a difference or anomaly compared with the long-term mean (1979–2019). This indicator complements ground-based measurements by using satellite observations that detect a freeze-thaw (FT) signal from microwave brightness temperature measurements that are sensitive to changes in the relative abundance of liquid water (e.g., soil moisture) at the land surface between frozen and non-frozen conditions. Previous studies using these observational data provide evidence of an increasing annual thaw cycle and general reduction in temperature constraints on vegetative growth over the Northern Hemisphere from regional climate warming (Kim et al., 2017a). Components of this indicator include:

- Number of unfrozen days per year in the contiguous 48 states (Figure 1).
- Number of unfrozen days per year in Alaska (Figure 2).

2. Revision History

April 2021:   Indicator published.

Data Sources

3. Data Sources

FT data were provided by Drs. Youngwook Kim and John Kimball of the University of Montana. The FT data were developed from the Nimbus-7 Scanning Multichannel Microwave Radiometer (SMMR) Pathfinder, Special Sensor Microwave Imager (SSM/I), and SSM/I Sounder (SSMIS) datasets (Armstrong et al., 2015; Knowles et al., 2000).

4. Data Availability

EPA obtained the data for this indicator from Dr. Youngwook Kim and Dr. John Kimball at the University of Montana. They published a paper detailing the development of an updated FT Earth system data

record, or FT-ESDR (Kim et al., 2017a, 2017b), and they provided EPA with a summary file containing annual unfrozen days for the contiguous 48 states, Alaska, and the contiguous 48 states plus Alaska. The current indicator represents version 042 of Kim and Kimball's dataset.

All raw source data are available for download in the form of satellite images. SMMR data and data descriptions are available on the web at: https://nsidc.org/data/nsidc-0071. SSM/I-SSMIS data and data descriptions are available on the web at: https://nsidc.org/data/nsidc-0032. The global FT-ESDR is archived and distributed for public access through the National Snow and Ice Data Center (NSIDC) at: https://nsidc.org/data/nsidc-0477/versions/4. There are no confidentiality issues that could limit accessibility.

Methodology

5. Data Collection

This indicator is based on the number of unfrozen days per year in the contiguous 48 states and Alaska. It was developed by analyzing satellite microwave brightness temperature (T_b) observations, which are sensitive to changes in the relative abundance of liquid water at the land surface between frozen and non-frozen conditions. This method specifically focuses on the condition of the land surface (frozen ground, where soil moisture is frozen). It is not limited to measuring the condition of open bodies of water; in fact, steps have been taken to avoid relying on map pixels that are dominated by large water bodies.

The authors developed the FT-ESDR using the SMMR, SSM/I, and SSMIS satellite sensor records:

- **SMMR (Knowles et al., 2000):** The SMMR onboard the Nimbus-7 Pathfinder satellite collected brightness temperature data from October 1978 to August 1987. The global data were collected at a resolution of 25 kilometers at five channels including 37 gigahertz (GHz) for both vertical and horizontal polarizations. The sensor collected data twice a day on alternate days (with no data collection on the intervening days) at local noon and local midnight. Documentation and more information on the data can be found at: https://nsidc.org/data/nsidc-0071#.

- **SSM/I-SSMIS (Armstrong et al., 2015):** The SSM/I and SSMIS instruments started collecting brightness temperature data in July 1987, and data collection continues today. The global data were collected at a resolution of 25 kilometers at four channels including 37 GHz for both vertical and horizontal polarizations (only vertical for 22 GHz). The sensors collect twice-daily data with overpasses at about 6:00 a.m. and 6:00 p.m. The SSM/I and SSMIS sensor series data consist of measurements from multiple instruments; the intercalibration and data processing are documented on their website (www.remss.com/support/known-issues/). Documentation and more information on the data can be found at: https://nsidc.org/data/nsidc-0032#.
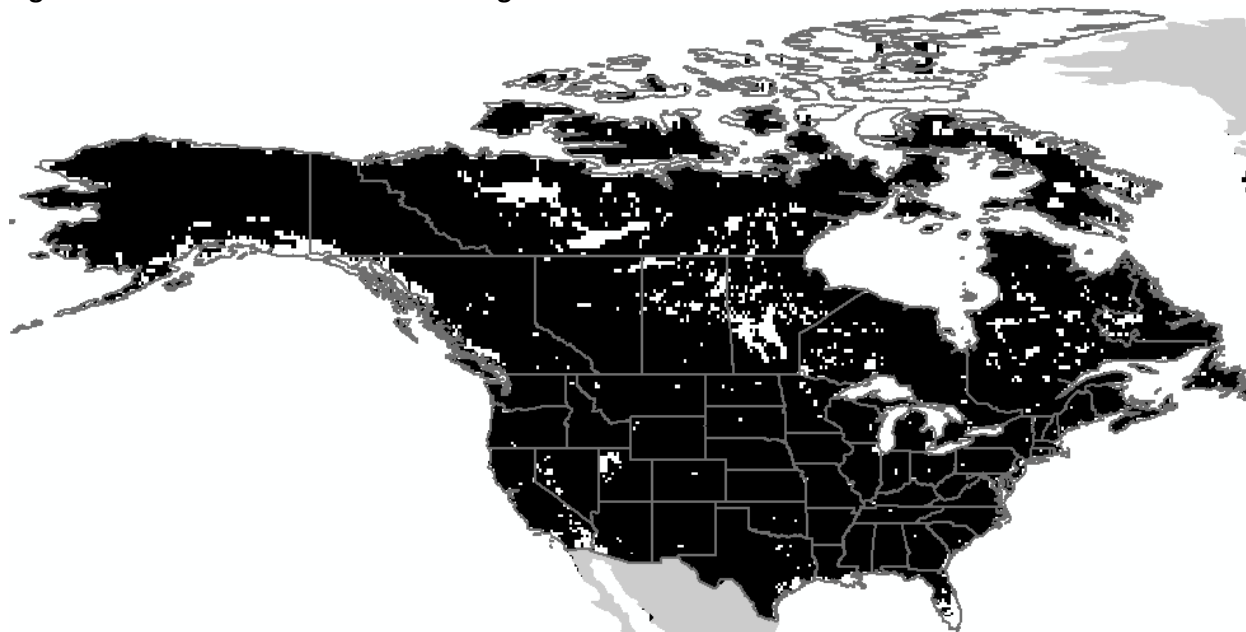
This satellite-based method offers a useful complement to other analyses that are based on air temperatures measured at weather stations. Air temperature data are widely used, quality controlled, and highly precise, so they are certainly a viable means to track temperature trends, as EPA has done in several of its other indicators. Nonetheless, this satellite-based method adds value because it enables detection of the FT status of the ground, and its coverage of the entire land surface means it can characterize the condition of locations that might not be well represented by the long-term weather

station network, due to the limits of station density and unique local topographic and microclimate conditions.

6. Indicator Derivation

The FT-ESDR was developed for land areas where the average number of days with freezing temperatures exceeds five per year based on surface air temperature (SAT) daily minima over a 36-year record (1979–2014). This indicator is also restricted to land areas with at least some vegetation, as defined from a MODIS land cover map, and limited to areas that are not permanently frozen. Thus, it excludes large water bodies and permanent ice/snow features. These considerations allow the analysis to focus on areas (covering most of the country) where FT cycles influence vegetative growth. Figure TD-1 shows areas that meet the requirement for at least five freezing days per year and were not excluded for other reasons described above.

Figure TD-1. Areas with Sufficient Chilling for Inclusion in This Indicator

This map shows the FT-ESDR domain for the United States and neighboring countries. White shading shows grid cells where data cannot be computed because there are fewer than five frozen days per year on average, or because the landscape is unvegetated, a large open water body, or permanently frozen. Black pixels represent the spatial domain covered by this indicator. Data source: Kim and Kimball, 2020.
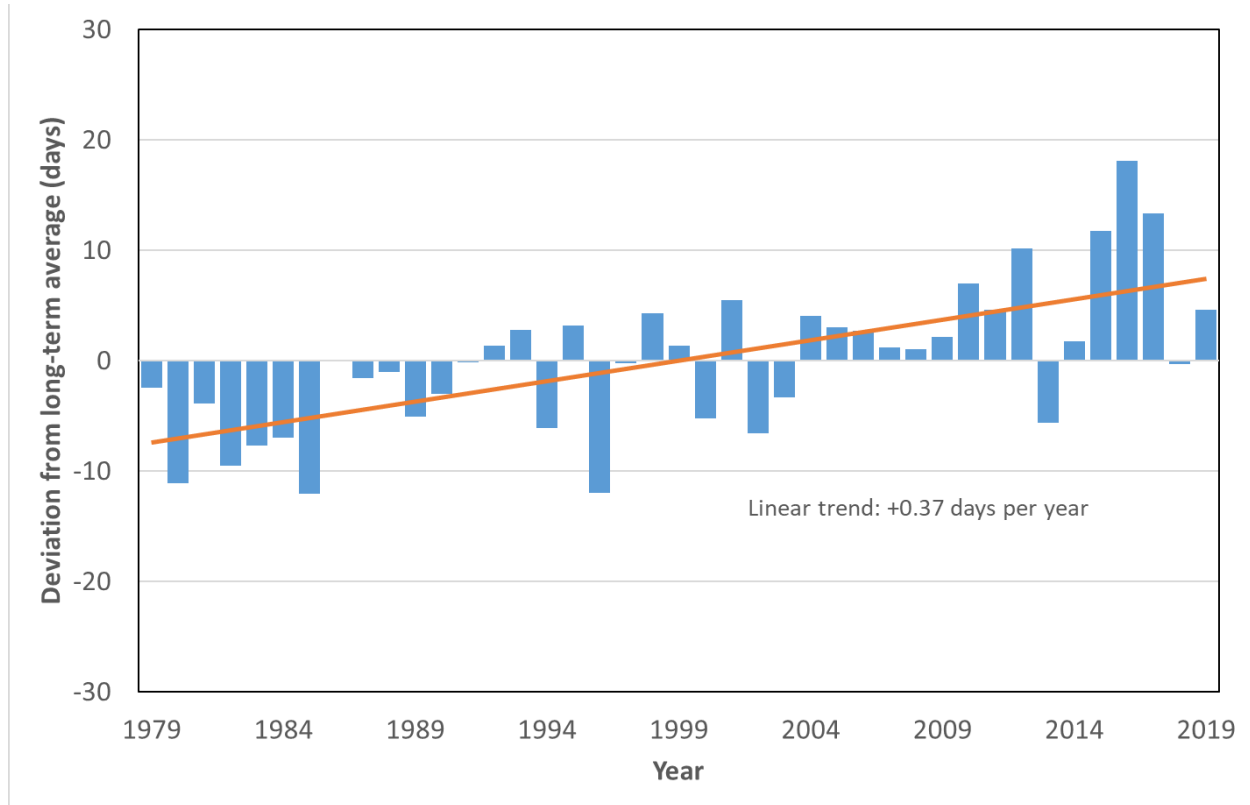
The annual grid-cell-wise FT classification thresholds were calculated separately for morning (a.m.) and evening (p.m.) satellite overpass T_b retrievals using corresponding daily minimum and maximum SAT measurements. The resulting a.m. and p.m. FT classifications were combined into a daily composite with four discrete classification levels. Each grid cell day in the FT-ESDR was assigned as frozen, non-frozen, transitional, or inverse transitional based on how the morning and evening brightness observations compared with their respective thresholds. Days with a.m. and p.m. frozen were assigned as frozen days; a.m. and p.m. thawed were non-frozen days; a.m. frozen and p.m. thawed were transitional days; and a.m. thawed and p.m. frozen were inverse transitional days. The resulting FT-ESDR, with FT values for each grid cell day in the 1979–2019 period, formed the basis for this indicator. Kim et al. (2017a) provide a complete description of the analytical procedures used to develop the FT-ESDR.

The data used in the indicator are derived from the global FT-ESDR, cropped to the shape of the contiguous 48 states and Alaska. The annual non-frozen season was defined from the daily FT-ESDR as the total number of non-frozen (a.m. and p.m. thawed) days per year. Non-frozen days averaged over all grid cells in the year within the contiguous 48 states and Alaska were used to determine annual non-frozen season anomalies. The anomalies were calculated as annual differences from the long-term mean based on the period of record (1979–2019).

Figures 1 and 2 show time series for the number of non-frozen days in a calendar year, for the contiguous 48 states and for Alaska. Each graph shows each year's deviation from the 1979–2019 long-term average, which is set at zero for a reference baseline. Thus, if year *n* shows a value of 4, it means that year had four more unfrozen days than usual. Note that the choice of baseline period will not affect the shape or the statistical significance of the overall trend; it merely moves the trend up or down on the graph in relation to the point defined as "zero."

For reference, Figure TD-2 shows the effect of combining the contiguous 48 states and Alaska into a single graph. The combined results naturally align more closely with the contiguous 48 states (Figure 1 of the indicator) because it has a much larger total land area than Alaska.

Figure TD-2. Number of Unfrozen Days in the Contiguous 48 States and Alaska, 1979–2019

This figure shows the number of unfrozen days in the contiguous 48 states and Alaska compared with the 1979–2019 average. For each year, the bar represents the number of days shorter or longer than average. Positive numbers represent years with more unfrozen days than average. The trend line represents an ordinary least-squares linear regression. Data source: Kim and Kimball, 2020.

The map in Figure 3 shows the long-term change in annual unfrozen days across North America (contiguous 48 states, Alaska, and Canada). This trend analysis uses methods described in Kim et al. (2012), including Sen's slope regression and Kendall's tau for significance. The annual rate of change was multiplied by the number of years to derive an estimate of total change. The color ramp accommodates the vast majority of observations (-40 to 40), a range that contains 99.2 percent of the pixels in the spatial domain. A few of the remaining pixels range up to nearly +100 unfrozen days.

7. Quality Assurance and Quality Control

Information on quality assurance (QA) and processing protocols for the SMMR dataset can be found at: https://nsidc.org/data/nsidc-0071. An analysis of processed data and expected residual errors may be found in Njoku et al. (1998). Information on QA and processing protocols for the SSM/I-SSMIS dataset can be found at: https://nsidc.org/data/nsidc-0032.

The development of the FT-ESDR involved extensive QA and quality control (QC) measures for assessing the reliability of the metric. The authors of Kim et al. (2017a) compared the FT-ESDR classifications with independent in situ daily minimum and maximum SAT measurements from 4,253 +/- 632 (interannual standard deviation) weather stations and generated a QA map of low and high relative mean annual classification accuracy. Manual inspection of this map (Figure 6 in Kim et al., 2017a; reproduced in Figure TD-1) shows the predominance of "good" (85–95 percent agreement) and "best" (>95 percent agreement) relative quality in the contiguous 48 states and Alaska. The authors of Kim et al. (2017a) also flagged other potential factors affecting FT classification agreement. They compared grid-cell-wise metrics of frozen season duration, primary spring thaw date, and non-frozen season duration against independent cryosphere data records and discussed reasons for discrepancy. These data came from the Global Lake and River Ice Phenology Database, annual ice breakup dates for the Tanana River in Alaska, and the NASA MEaSUREs Greenland surface melt record.

Readers can find more details in Kim et al. (2017a), which contains detailed results of the QA assessment and comparison against independent data. Estimated annual QA maps and grid-cell-level daily QC flag information is included with the global FT-ESDR database distributed through NSIDC (Kim et al., 2017b).

Analysis

8. Comparability Over Time and Space

All the satellite instruments used for this indicator have collected data in a consistent manner worldwide. However, there have been some differences in collection and data processing over time. The team that developed this indicator has taken several steps to adjust for these differences and ensure that the resulting data can be compared credibly over the entire period of record.

The SMMR data were collected at a frequency of two days. Time gaps in data also occurred, as described in more detail in the "Limitations of the Data" section of the data documentation: https://nsidc.org/data/nsidc-0071. Ground track errors, also described in the preceding link, resulted in small errors (on the order of 0.1 °C) for January 1981 through May 1983. The missing T_b data attributed to orbital gaps between satellite overpasses were filled on a grid-cell-wise basis by linear interpolation of temporally adjacent, successful T_b retrievals to generate spatially and temporally consistent daily (AM and PM overpass) T_b observations (Kim et al., 2011). The FT-ESDR contains QC flags that are spatially and

temporally dynamic and assigned on a per-grid-cell basis to denote missing satellite T_b records that are subsequently gap-filled through temporal interpolation of adjacent T_b retrievals prior to the FT classification (Kim et al., 2017b).

The SSM-I/SSMIS data may contain geolocation errors in input Remote Sensing Systems swath data of up to 10 km and additional error from nearest-neighbor interpolation from the over-sampled array of approximately 6 km. Additionally, the SSM/I and SSMIS sensor series data consist of measurements from multiple instruments, but steps were taken to harmonize these measurements through intercalibration. These processing steps are documented at: www.remss.com/support/known-issues.

The SMMR and SSM/I-SSMIS datasets also have differing data collection and processing methodologies, as described in more detail in their respective documentation: https://nsidc.org/data/nsidc-0071 and: https://nsidc.org/data/nsidc-0032. For SMMR, the two sensor overpass times are midnight and noon, and data were collected on alternate days; the SSM/I and SSMIS sensors have overpass times at approximately 6 AM and 6 PM and collect daily measurements. The authors developed annual FT thresholds separately for AM and PM overpasses. For most years in the FT-ESDR, the annual thresholds were developed from data with consistent satellite image collection times, which would account for the change in measurement collection times across years. However, 1987 FT-ESDR data are based on measurements from both SMMR and SSM-I/SSMIS, which may affect the accuracy of the FT-ESDR data for that year because the AM and PM FT thresholds were calibrated on measurements at different times of the day. Before determining AM and PM FT classification thresholds for each grid cell by empirical linear regression between model reanalysis daily SAT and satellite T_b retrievals, the SMMR record was matched to the SSM/I record using pixel-wise adjustment of the SMMR and SSM/I T_b measurements for 1987 to ensure cross-sensor consistency (Kim et al., 2012).

Care has been taken to account for missing data, and thereby prevent missing data from biasing the resulting annual averages. According to Kim et al. (2017a), on average, annual satellite records were missing data for 34.3 +/- 24.3 percent of the relevant land area due to orbital gaps between satellite overpasses. To generate the FT-ESDR, these spatial data were filled on a grid-cell-wise basis by linear interpolation of temporally adjacent, successful T_b retrievals based on peer-reviewed methods (Kim et al., 2011). The authors also interpolated large gaps of missing data in January and December 1987 and January 1988 using empirical relationships developed from ERA-Interim (Dee et al., 2011) global model reanalysis SAT and satellite T_b data records. In 2020, a new ERA5-based calibration (instead of ERA-Interim) was applied to the entire record. It verified consistent performance relative to the prior (v04) record and global weather station observations.

The grid-cell-wise T_b threshold and annual calibration used for the FT classification algorithm reduce the potential influence of spatial and temporal variations in climate and land surface conditions on FT classification accuracy, and promote greater compatibility in global product performance over the long-term record (Kim et al., 2017a).

9. Data Limitations

Factors that may impact the confidence, application, or conclusions drawn from this indicator are as follows:

1. The agreement of the FT-ESDR with in situ temperature measurements is not perfect, as described in Section 10. However, the FT-ESDR is well tested and provides a reasonably reliable complement to ground-based data.

2. The FT classification accuracy was found to be inversely proportional to the spatial fraction of open water bodies (F_w) within a grid cell. The FT ESDR QC flags distinguish grid cells with large open water areas ($F_w > 0.2$) (Kim et al., 2017a).

10. Sources of Uncertainty

Many factors can diminish the accuracy of satellite detection of FT status. These factors include terrain type; number of SAT validation stations; length of seasonal transitions; and land surface heterogeneity, including presence of surface water and terrain complexity. Time of day of measurements also influences agreement with SAT records. Thus, the agreement between the FT-ESDR and in situ SAT measurements varies, with an average agreement of 90.3 +/- 1.4 percent (inter-annual standard deviation) for the PM overpass and 84.3 +/- 1.7 percent (inter-annual standard deviation) for the AM overpass. The discrepancy may be attributed to spatial mismatch between the in situ weather station observations and overlying coarser satellite footprint. See Kim et al. (2017a) for further discussion of factors affecting FT classification agreement.
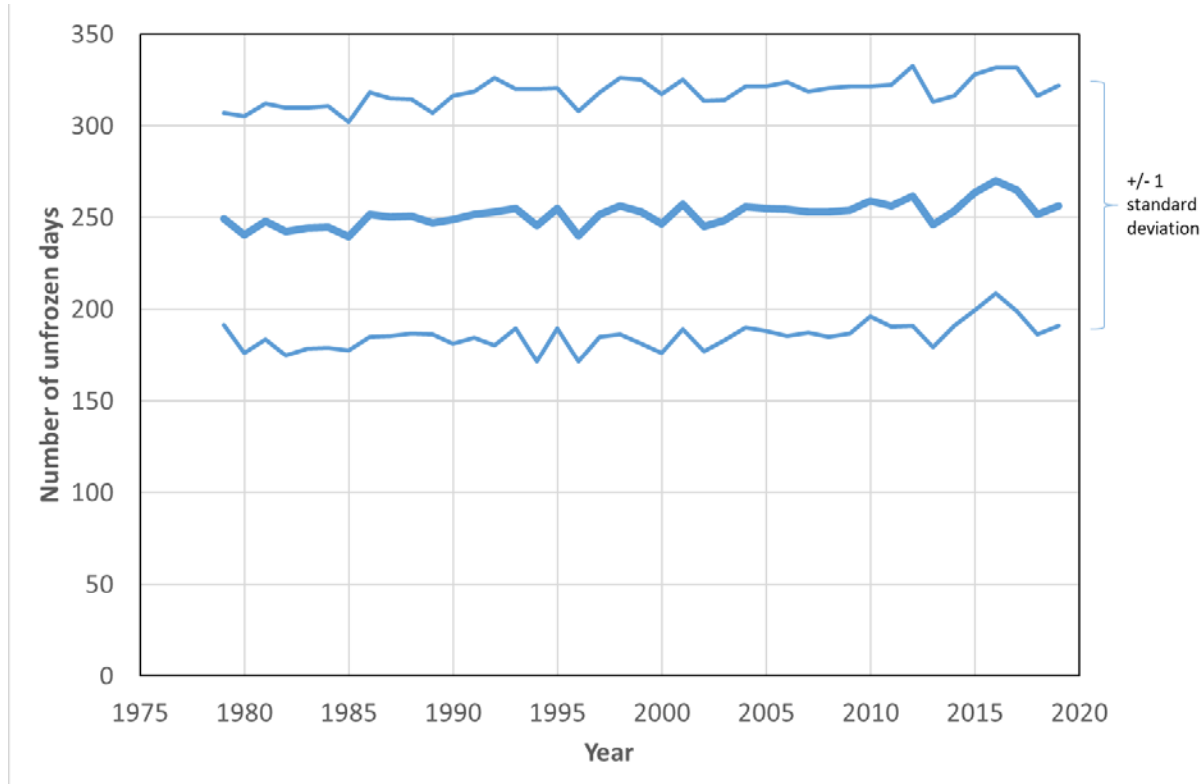
The authors interpolated to fill in gaps in data, and this may present a source of uncertainty in the overall trend. Changes in measurement techniques over time and satellite measurement instrument errors also contribute to uncertainty.

11. Sources of Variability

At any given location, the number of days experiencing frozen conditions naturally varies from year to year as a result of normal variation in weather patterns, multi-year climate cycles such as the El Niño–Southern Oscillation and Pacific Decadal Oscillation, and other factors. Overall, this type of variability should not impact the conclusions that can be inferred from the trends shown in this indicator.

There is also inherent variability over space in any given year, as this indicator is aggregated over a wide variety of climate zones. To give readers a sense of this natural geographic variation, Figure TD-3 shows the absolute number of unfrozen days per year (the spatial mean) along with lines that indicate one standard deviation in each direction to suggest the spread of the distribution. Figure TD-3 shows that the average annual number of unfrozen days across the entire coverage area is approximately 250, but there is a substantial geographic spread. If one were to assume an approximately normal distribution, one would infer that about 68 percent of the grid cells on the map had a number of unfrozen days that fell between the upper and lower bounds shown in Figure TD-3.

Figure TD-3. Number of Unfrozen Days in the Contiguous 48 States and Alaska, 1979–2019, with Standard Deviation Showing Geographic Variation
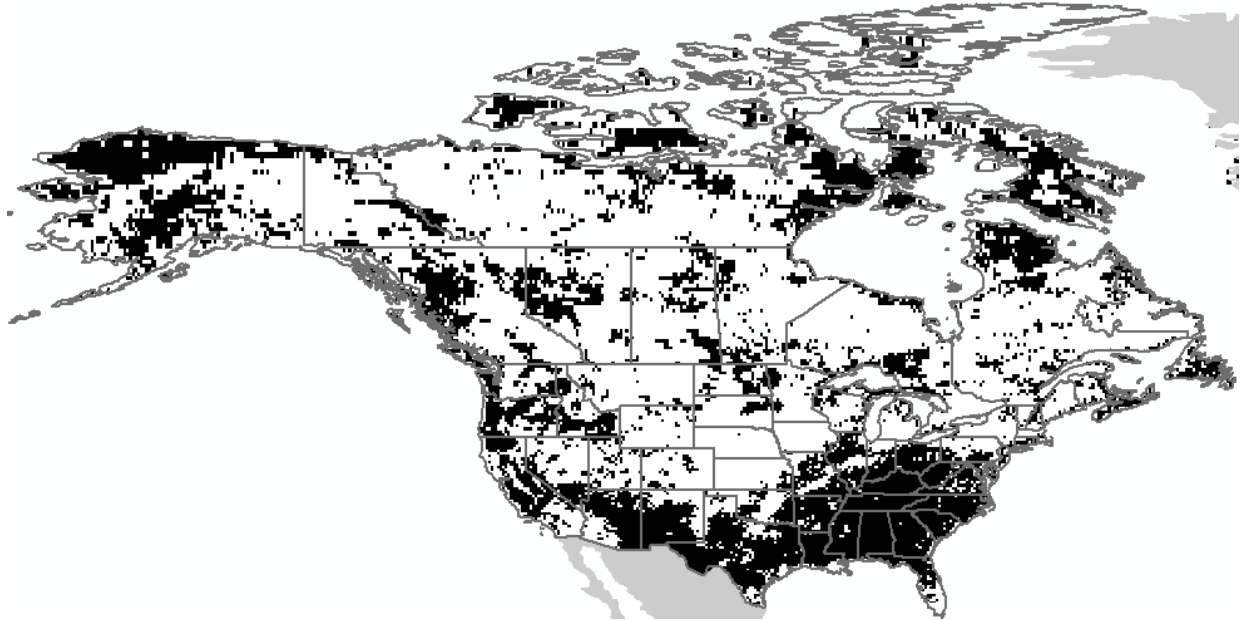

This figure shows the average annual number of unfrozen days in the contiguous 48 states and Alaska. Upper and lower bounds represent one standard deviation on either side of the mean. Data source: Kim and Kimball, 2020.

12. Statistical/Trend Analysis

The figures in this indicator show annual data points and do not attempt to present multi-year trends. However, a simple analysis of trends via ordinary least-squares linear regression indicates that the annual number of unfrozen days increased over time between 1979 and 2019 in the contiguous 48 states (+0.37 days per year, $p < 0.0001$) and in Alaska (+0.39 days per year, $p = 0.002$). The combined contiguous 48 states/Alaska time series in Figure TD-2 shows an increase of +0.37 days per year ($p < 0.0001$). As the p-values indicate, these changes are statistically significant to a 95 percent level. The map in Figure TD-4 shows which individual pixels had statistically significant trends, based on the Sen's slope/Kendall's tau trend analysis discussed in Kim et al. (2012). This analysis used $p < 0.1$ (a 90 percent level) as the criterion for significance.

Figure TD-4. Significance of 1979–2019 Trends in the Annual Number of Unfrozen Days

This map shows where long-term trends in unfrozen days are statistically significant. Pixels with p < 0.1 (i.e., significant to a 90 percent level) are shaded black. Data source: Kim and Kimball, 2020.

References

Armstrong, R., K. Knowles, M. Brodzik, and M.A. Hardman. 2015. DMSP SSM/I-SSMIS Pathfinder daily EASE-Grid brightness temperatures, Version 2 (1987–2014). NASA DAAC at the National Snow and Ice Data Center. http://nsidc.org/data/nsidc-0032.html.

Dee, D.P., et al. 2011. The ERA-Interim reanalysis: Configuration and performance of the data assimilation system. Q. J. Roy. Meteorol. Soc. 137:553–597.

Kim, Y., and J. Kimball. 2020 update to data originally published in: Kim, Y., J.S. Kimball, J. Glassy, and J. Du. 2017. An extended global Earth system data record on daily landscape freeze-thaw status determined from satellite passive microwave remote sensing. Earth Syst. Sci. Data 9:133–147.

Kim, Y., J.S. Kimball, K.C. McDonald, and J. Glassy. 2011. Developing a global data record of daily landscape freeze/thaw status using satellite passive microwave remote sensing. IEEE Trans. Geosci. Rem. Sens. 49:949–960.

Kim, Y., J.S. Kimball, K. Zhang, and K.C. McDonald. 2012. Satellite detection of increasing northern hemisphere non-frozen seasons from 1979 to 2008: Implications for regional vegetation growth. Remote Sens. Environ. 121:472–487. doi:10.1016/j.rse.2012.02.014

Kim, Y., J.S. Kimball, J. Glassy, and J. Du. 2017a. An extended global Earth system data record on daily landscape freeze-thaw status determined from satellite passive microwave remote sensing. Earth Syst. Sci. Data 9:133–147. doi:10.5194/essd-9-133-2017

Kim, Y., J.S. Kimball, J. Glassy, and K.C. McDonald. 2017b. MEaSUREs global record of daily landscape freeze/thaw status, version 4. NASA DAAC at the National Snow and Ice Data Center. doi:10.5067/MEASURES/CRYOSPHERE/nsidc-0477.004

Knowles, K., Njoku, E. G., Armstrong, R., and Brodzik, M. 2000. Nimbus-7 SMMR Pathfinder daily EASE-Grid brightness temperatures (1979–1987). NASA DAAC at the National Snow and Ice Data Center. http://nsidc.org/data/nsidc-0071.html.

Njoku, E.G., B. Rague, and K. Fleming. 1998. Nimbus-7 SMMR Pathfinder brightness temperature data. NASA Jet Propulsion Laboratory Publication 98-4.

USGCRP (U.S. Global Change Research Program). 2018. Impacts, risks, and adaptation in the United States: Fourth National Climate Assessment, volume II. Reidmiller, D.R., C.W. Avery, D.R. Easterling, K.E. Kunkel, K.L.M. Lewis, T.K. Maycock, and B.C. Stewart (eds.). www.globalchange.gov/nca4.

Weltzin, J., et al. 2020. Seasonality of biological and physical systems as indicators of climatic variation and change. Climatic Change 163:1755–1771. doi:10.1007/s10584-020-02894-0